

Low-lying S-wave and P-wave Dibaryons in a Nodal Structure Analysis

Yu-xin Liu^{1,3,4}, Jing-sheng Li¹, and Cheng-guang Bao^{2,4}

¹ Department of Physics, Peking University, Beijing 100871, China

² Department of Physics, Zhongshan University, Guangzhou 510275, China

³ Institute of Theoretical Physics, Academia Sinica, Beijing 100080, China

⁴ Center of Theoretical Nuclear Physics, National Laboratory of
Heavy Ion Accelerator, Lanzhou 730000, China

November 13, 2018

Abstract

The inherent nodal surface structure analysis approach is proposed for the six-quark clusters with u , d and s quarks. The wave-functions of the six-quark clusters are classified, and the contribution of the hidden-color channels are discussed. The quantum numbers and configurations of the wave-functions of the low-lying dibaryons are obtained. The states $[\Omega\Omega]_{(0,0+)}$, $[\Omega\Omega]_{(0,2-)}$, $[\Xi^*\Omega]_{(1/2,0+)}$, $[\Sigma^*\Sigma^*]_{(0,4-)}$ and the hidden-color channel ones with the same quantum numbers are proposed to be the candidates of experimentally observable dibaryons.

PACS Numbers: 14.20.Pt, 03.65.Fd, 11.30.-j, 21.60.Gx

1 Introduction

It has been known that quark degrees of freedom are essential to describe properties of hadrons and the quantum chromodynamics(QCD) is the underlying theory for strong interaction. One of the current issues in this field involves the attempt to derive the short-range part of the nucleon-nucleon interaction from the quark-gluon degrees of freedom. Unfortunately, it is now very difficult to make quantitative predictions with QCD at low and intermediate energy region. Therefore various phenomenological models based on the QCD assumptions, such as bag models[1], cluster model[2] have been developed.

With the MIT bag model, a dibaryon, namely the H particle, was predicted by Jaffe in the later of 1970's[3]. Thereafter many attempts have been made to search for dibaryons in both theory and experiment, because it is an appropriate place to investigate the quark behavior in short distance and to explore the exotic states of QCD. On the theoretical side, almost all QCD inspired models (see for example Refs.[4, 5, 6, 7, 8, 9]), even the QCD sum rules[10] and lattice QCD[11] predict that there exist dibaryon states. However, no dibaryon state except for the deuteron has been well established in experiment up to now. On the other hand, the theoretical predictions are quite far away from each other, since different approaches take different models and interactions (at least the interaction strength).

After Jaffe predicted the existence of the H particle(strangeness $s = -2$, $J^P = 0^+$) as a color-singlet multi-quark system($q^m\bar{q}^n, n + m > 3$), Harvey developed a method in cluster model[12], with which all the antisymmetric six-quark states with definite orbital and isospin-spin symmetries were classified. Meanwhile, many hidden-color channel states which can not be represented in terms of free baryons were found. Unfortunately, the constituents Harvey considered include only u and d quarks. In other words, the strangeness of the system has not yet been taken into account. However, more and more evidences proved that the system with non-zero strangeness may be more stable to exist as a dibaryon(see for example Refs.[6, 8, 9, 13, 14]). It is then necessary to extend Harvey's framework to include s quarks and get a complete result.

Along the way of the non-relativistic QCD, the concept of wave-function can be implemented to describe many-quark states, and embodied in the non-relativistic quark model[12, 15]. On the other hand, it has been known that analyzing the symmetric property and the inherent nodal surface[16, 17, 18] is a quite powerful approach to investigate few-body electron and nucleon systems. To neglect handling the complicated strong interactions of the six-quark system in QCD and obtain model independent result, we will then study the dibaryon states by extending Harvey's algebraic framework and analyzing the inherent nodal surface of the system in this paper.

This paper is organized as follows. Following this introduction, the symmetry of the six-quark cluster which may include u , d and s quarks will be analyzed in Section 2. In Section 3, the quantum numbers of the possible six-quark states will be discussed systematically by analyzing the inherent nodal surface structure of the system. In Section 4 and Section 5, we discuss the low-lying S-wave and P-wave states and the perspective to search for dibaryons, respectively. Finally, a summary and some remarks are given in Section 6.

2 Symmetries of the Six-quark States

The wave-function of six-quark systems can be written as the coupling of an orbital part and an internal part, fulfilling the requirement that the total wave-function must be antisymmetric, i.e. has a symmetry $[1^6]$. It has been well known that the system with u , d and s quarks possesses the internal symmetry $SU_{CFS}(18) \supset SU_C(3) \otimes SU_F(3) \otimes SU_S(2)$. Let $[f]_O$, $[f]_C$ and $[f]_{FS}$ be the irreducible representations (irreps) of the groups associated with the orbital, color and flavor-spin space, respectively, we shall have

$$[1^6] \in [f]_O \otimes [f]_C \otimes [f]_{FS}. \quad (1)$$

Although six-particle system in general does not impose any constraint on the orbital wave-function, which may have any one of the symmetries listed in the first column of Table 1, we should determine which choices are more favorable to binding and therefore

more probable to exist as low-lying states.

The irrep $[f]_{CF_S}$ of the $SU(18)$ can be reduced to $[f]_C$ of $SU_C(3)$ and $[f]_{FS}$ of $SU_{FS}(6)$ with the standard method[19]. The lack of direct experimental observation of free ‘‘color charge’’ suggests that not only the free baryons but also all the other observable states should be $SU(3)$ color singlet. We can thus restrict our study of six-quark systems to those having color symmetry

$$[f]_C = [2\ 2\ 2]. \quad (2)$$

Then we get the possible irreps $[f]_{FS}$ as listed in Table 1.

It has been known that u , d and s quarks can construct eight free baryons: N , Δ , Σ , Σ^* , Λ , Ξ , Ξ^* and Ω . All of them are the building blocks of the dibaryons and have flavor-spin symmetry $[f]_{FS}=[3]$. Thus it is reasonable to assume that the low-lying dibaryon states which can be observed in experiments may have symmetry

$$[f]_{FS} \in [3] \otimes [3] = \{[6], [5\ 1], [4\ 2], [3\ 3]\}. \quad (3)$$

These particular symmetries are shown by an asterisk in Table 1 for latter reference.

According to the subclassification of the symmetry $SU_{FS} \supset U_s(1) \otimes SU_T(2) \otimes SU_S(2)$, we list the strangeness, isospin and spin for the six-quark systems in Table 2, where both the two-baryon bound states and the hidden-color channel states (marked with CC) are listed. Table 2 shows that there exist many hidden-color channel states in the six-quark systems, whose $SU_{FS}(6)$ symmetry are the same as those of the two-baryon states. Furthermore, all the states of the $SU_{FS}(6)$ symmetries without asterisks in Table 1 are also ‘‘hidden-color’’ states in the cluster representation.

Furthermore, as a constituent of the low-lying dibaryons, each baryon is assumed to be in its ground state. It turns out that all these ground states have orbital symmetry $[f]_O = [3]$. It follows that in the cluster model, we can consider the six-quark system whose orbital wave-functions hold the symmetry

$$[f]_O \in [3] \otimes [3] = \{[6], [5\ 1], [4\ 2], [3\ 3]\}, \quad (4)$$

if only the two-baryon bound states are taken into account. If we include the hidden-color channel states, the other orbital symmetries should consequently be deliberated.

The realistic configuration of the orbital wave-functions should be fixed with the intrinsic property of the system.

3 Nodal Structure Analysis of Low-lying Six-quark States

The Schrödinger equation of multi-particle system can be written as:

$$H\psi(\xi) = E\psi(\xi), \quad (5)$$

where ξ is the set of variables, such as coordinates, spins and isospins. If G is the symmetry group of the Hamiltonian H , in other words, H is invariant to the transformation \hat{O} which is an element of the group G , the eigenstates of the Hamiltonian can be classified with the irreducible representation of G .

On the other hand, It has been known that if a state contains excited spatial oscillations (i.e., the orbital wave function contains nodal surfaces if observed in a body frame), it would be higher in energy than the states not containing excited oscillations. For example, the energy and the number n of nodals of the states in one-dimensional infinite wall is $E_n = \frac{\pi^2 \hbar^2 (n+1)^2}{2ma^2}$, where a is the width of the wall and m is the mass of the particle. Moreover, It has been found that there are two kinds of nodal surfaces. The first kind of them depends on dynamics, while the second relies purely on symmetry. It means that the second kind nodal surfaces are inherently contained in certain wave functions. Let Ψ be an eigenstate of a quantum system, \mathcal{A} denote a geometric configuration, in some cases \mathcal{A} may be invariant to a specific operation \hat{O} , we have then

$$\hat{O}\Psi(\mathcal{A}) = \Psi(\hat{O}\mathcal{A}) = \Psi(\mathcal{A}). \quad (6)$$

For example, when \mathcal{A} is a regular octahedron (OCTA, see Fig. 1) for a 6-body system, \mathcal{A} is invariant to a rotation about a 4-fold axis of the OCTA by 90° together with a cyclic permutation of the particles 1, 2, 3 and 4. According to the representations of the operation on Ψ , Eq. (6) can always be written in a matrix form and appears as a set of

homogeneous linear equations. It is apparent that, whether there exists nonzero solution of $\Psi(\mathcal{A})$, in other words, whether the state Ψ is accessible to the configuration \mathcal{A} , depends on the inherent symmetric property of the configuration. The symmetry imposes then a very strong constraint on the eigenstate so that the Ψ may be zero at \mathcal{A} . It indicates that there may exist a specific kind nodal surface, that is imposed by the intrinsic symmetry of the system (fixed at body-frames) and independent of the dynamical property at all. One usually refers such kind nodal surface (the second kind nodal surface mentioned above) as inherent nodal surface (INS). It is apparent whether the INS would appear is crucial to the low-lying energy spectrum of a quantum system. The inherent nodal surface structure analysis approach has then been proposed for few-body electron and nucleon systems[16, 17, 18].

For a six-quark system, the orbital wave function may contain many components. Each of them is specified by a set of quantum numbers of inherent symmetry. Denoting λ as a representation of the permutation group S_6 , i a basis function of this representation, M the Z -component of L , and g other quantum numbers, we can express the components of the wave-function as $F_{LMg}^{\lambda,i}(1 \cdots 6)$. Defining a body-frame, we have the relation

$$F_{LMg}^{\lambda,i}(1 \cdots 6) = \sum_Q D_{QM}^L(-\gamma, -\beta, -\alpha) F_{LQg}^{\lambda,i}(1' \cdots 6'), \quad (7)$$

where D_{QM}^L is an element of the matrix of rotation, α , β and γ are the Euler angles specifying the orientation of the body-frame, Q denotes the projection of L along the third body-axis, $(1 \cdots 6)$ and $(1' \cdots 6')$ stand for that the coordinates are relative to the laboratory frame and to the body-fixed frame, respectively. By analyzing the inherent nodal surface structure of the system, we shall figure out which components are advantageous to binding and thereby dominate the low-lying states in what follows.

The symmetric operation on a system includes usually rotation, space inversion, permutation of the particles, and so on. According to the theory of space group, we can classify the rotation axes into two kinds. If a geometric configuration contains a m -fold axis of the first kind, the shape would be invariant with respect to a rotation about the axis by the angle $\frac{2\pi}{m}$. If it involves a m -fold axis of the second kind, the shape would

be invariant with respect to the rotation together with a space inversion. In general, a configuration containing at least one m -fold axis ($m \geq 2$) is called a symmetric configuration. The spatial symmetry of a geometric configuration is specified by the m -fold axes contained in the configuration. For a six-quark system, there are many symmetric configurations located everywhere in the coordinate space. However, as a quantum system, not all the symmetric configurations are allowed, since some of them might be prohibited by the emergence of the INS.

As an example, let OO' be a 3-fold axis of a 6-body configuration as shown in Fig.1, one can easily realize that a rotation about OO' by 120° is equivalent to the cyclic permutation of particles 2, 5, 3 and that of 1, 4, 6, respectively (see the figure). We have then

$$\hat{P}(253)\hat{P}(146)\hat{R}_{-120^\circ}^{OO'}F_{LQg}^{\lambda,i}(1' \cdots 6') = F_{LQg}^{\lambda,i}(1' \cdots 6'). \quad (8)$$

The crucial point is that $F_{LQg}^{\lambda,i}$ is a basis function of representations of both the spatial rotation group and the permutation group. Hence, as the matrixes of representation of the two operators are known, Eq. (8) can be written in a matrix form, and appears as a set of homogeneous linear equations. It is well known that homogeneous equations might not have nonzero solutions, which depends on whether the determinant of the matrix is zero. The determinant depends on the λ and L . Once the determinant is nonzero, all the $F_{LQg}^{\lambda,i}$ (all i and Q) must be zero at this symmetric configuration disregarding the size of the shape and the permutation of the particles at the vertexes of the shape. In other words, an inherent nodal surface appears in these components of the symmetric configuration. These components are then prohibited to get access to this shape.

Incidentally, if the m -fold axis belongs to the second kind, the constraint becomes

$$\hat{\mathbf{I}}\hat{P}\hat{R}F_{LQg}^{\lambda,i}(1' \cdots 6') = F_{LQg}^{\lambda,i}(1' \cdots 6'), \quad (9)$$

where $\hat{\mathbf{I}}$ is the operator of space inversion.

Among all the symmetric configurations of a six-body system, the one having the highest geometric symmetry (i.e., having the most m -fold axes) is the regular octahedron (OCTA) as shown in Fig.1, where three 4-fold axes, four 3-fold axes, and six 2-fold axes

are contained. Since each m -fold axis would cause a constraint, evidently the OCTA is strongly constrained by symmetry. Only a small portion of quantum wave-functions with specific λ and L can get access to it (i.e., the wave function is nonzero at it). The accessibility of the OCTA turns out to be an important point. Once the OCTA is accessible to a wave function, all the symmetric configurations with a lower geometric symmetry in the neighborhood of the OCTA (for example, the prolonged-octahedron with the shape being prolonged along k' , the deformed-octahedron with the particles 1, 2, 3 and 4 illustrated in Fig. 1 forming a rectangle or a diamond) are also accessible to the wave-function. Consequently, the wave-function is able to distribute in a large domain including the OCTA inside and free from the intervention of the INS. Such a case is highly favorable to binding. Whereas if a wave function contains an INS, its energy will increase drastically.

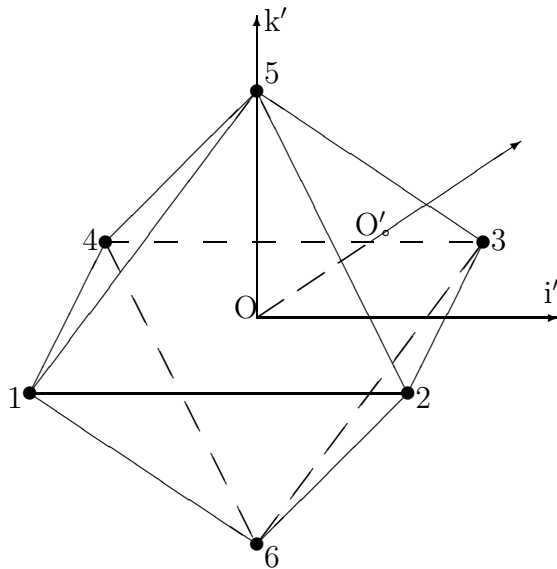


Fig. 1 The regular octahedron.

The configuration with the second strongest geometric symmetry is that the positions of the six quarks form a regular pentagon pyramid(PENTA, shown as Fig.2). In an extreme case, the PENTA can be C-PENTA, which corresponds to that with $h = 0$

in Fig. 2. It is evident that, if the C-PENTA is accessible, all the lower symmetric configurations in its neighborhood (for instance, the PENTA) are also accessible, since the restraints imposed by the configuration are much weaker.

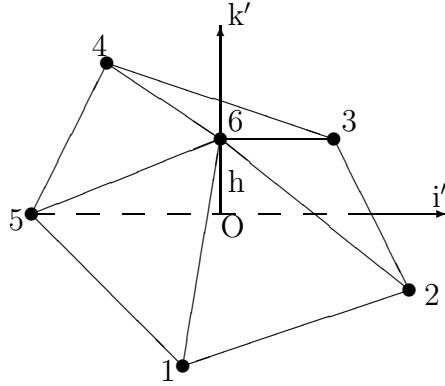


Fig. 2 The regular pentagon pyramid.

It is evident that if a state does not contain a collective excitation of rotation, i.e., the angular momentum L is zero, it would be usually lower in energy than the state with $L \neq 0$. This is particularly true for the systems with a very small size whose energy $E \propto \frac{L(L+1)}{r^2}$. On the experimental side, it has been found that the ground states of 4 particles and 6 particles are always composed of components with $L=0$, while the resonances with $L \geq 1$ have quite higher excitation energies (for a recent data compilation see Ref.[20]). It is then reasonable to assume that the low-lying states of the six-quark system consist of components with $L = 0$. Furthermore, the above discussion shows that all the low-lying states in quantum mechanics are mainly composed of nodeless components. Therefore, if we limit the problem to the low-lying states, it is an appropriate way to consider the S-wave nodeless components. However, in view of the nucleon-nucleon collision, the P-wave resonance may also be important.

Taking the way developed in Ref.[18], we obtain the nodeless accessibility (i.e. number of the wave-functions) of the configurations OCTA and C-PENTA with $L^\pi = 0^+, 1^-$ and the possible spatial permutation symmetry S_6 . The result is that only the irreps

$$[f]_O = \{\lambda\} \in \{[6], [42], [222]\} \quad (10)$$

of the S_6 for the S-wave states, and

$$[f]_O = \{\lambda\} \in \{[5\ 1], [4\ 1\ 1], [3\ 3], [3\ 2\ 1], [2\ 2\ 1\ 1]\} \quad (11)$$

for the P-wave resonance are nodeless accessible to both the OCTA and the C-PENTA configurations.

It has been shown that the sources of INS may exist in the quantum states. Nonetheless, there are essentially inherent-nodeless components of wave-functions (each with a specific set of (L^π, λ)). The identification of these particularly favorable components is a key to understand the low-lying spectrum. Taking the standard method of irreducible representation reduction, we get the quantum number spin(S), isospin(T), total angular momentum(J) and strangeness(s) of the S-wave states ($L^\pi = 0^+$) with S_6 irreps $[6]$, $[4\ 2]$, $[2\ 2\ 2]$ and those of the P-wave states ($L^\pi = 1^-$) with S_6 irreps $[5\ 1]$, $[4\ 1\ 1]$, $[3\ 3]$, $[3\ 2\ 1]$, $[2\ 2\ 1\ 1]$. The obtained accessibility is listed in Table 3 for the S-wave states and in Table 4 for the P-wave states, respectively.

4 The low-lying S-wave states

From the above discussion, we find that, when a wave-function $\Psi_{LS\lambda}$ possesses quantum numbers $(L^\pi\lambda) = (0^+[6])$, $(0^+[4\ 2])$, $(0^+[2\ 2\ 2])$, it can access both the OCTA and the C-PENTA. These and only these $\Psi_{LS\lambda}$ are inherently nodeless components in the two most important spatial configurations. They should then be the dominant components of the S-wave low-lying states.

Because INS have no relation with dynamics, we can discuss the low-lying states along the same line as that to discuss the nucleus ${}^6\text{Li}$ [18]. Comparing the symmetry of the dibaryons ($S_6 \otimes \text{SU}_{CFS}(18)$) with that of the nucleus ${}^6\text{Li}$ ($S_6 \otimes \text{SU}_{TS}(4)$), one can easily infer that these two kind six-body systems have the same geometric configurations. According to the energy spectrum of ${}^6\text{Li}$, we can reach a conclusion that the states associating with orbital symmetries $[4\ 2]$ and $[2\ 2\ 2]$ have lower energies than those with only $[2\ 2\ 2]$ symmetry. Extending the results to include the spatial symmetry $[6]$, we can compare the

energies of the states and deduce the low-lying ones.

4.1 The states with strangeness 0

From the above discussion we obtain that only the $(L^\pi, [f]_O) = (0^+, [6])$ and $(0^+, [42])$ components are nodeless accessible to the S-wave states. If the hidden-color channel states are taken into account, the $(0^+, [222])$ component is also allowed. From Table 3, one can realize that the {isospin, spin} configurations $(T, S) = (0, 1), (1, 0), (1, 2), (2, 1)$ are the favorable ones since they are nodeless accessible to all the four orbital-{isospin, spin} configurations. Meanwhile, the states with $(T, S) = (0, 3), (3, 0)$ may also be the low-lying dibaryon states since their nodeless accessibility is the second largest one.

For the state with quantum number $(T, S) = (0, 1)$, both the $[6]$ and $[42]$ components are available. Therefore, two $T(J^\pi) = 0(1^+)$ partner states would be generated. Each of them is a specific mixture of the $[6]$ and $[42]$ components. According to Harvey's result[12], we know one of them is the deuteron whose dominant orbital symmetry is $[42]$. Of course, this is the lightest stable dibaryon. Because of the interference between the $[6]$ and $[42]$ components, there would be a gap between the partner states. The interaction is spin-dependent and complicated, but we can expect this gap to be large since even now there is no evidence for the existence of the partner of deuteron. Furthermore, since the $[222]$ component is also accessible, there may exist a hidden-color channel state with $(T, S) = (0, 1)$.

Referring to the order of states determined by considering the color-magnetic interaction between quarks in quark models[3], we expect that, besides deuteron, the $(T, S) = (1, 0)$ state with dominant orbital symmetry $[42]$ is the second lightest one, since it has small spin and isospin. From Table 2 we know that it is mainly a NN dibaryon. Since this state obeys the Pauli principle of two-nucleon systems $((-1)^{L+S+T} = -1)$, it may decay into two protons if its energy is not low enough. Then the possibility for it to be a stable bound state may be not very large. Meanwhile, the $T(J^\pi) = 1(0^+)$ state also has a partner with dominant orbital symmetry $[6]$. This state must have an energy much

higher than the $[42]$ component, it will be more easily to decay, so we do not discuss it at all.

Our result for the states with low isospin and spin is similar to that given in the quark-delocalization and color-screening model (QDCSM)[21, 22], where it was concluded that, besides deuteron, $(T, S) = (1, 0)$ and $(1, 1)$ are the next two lowest states and $(1, 0)$ may be even a stable dibaryon if the interaction is suitable. With regard to the state with $(T, S) = (0, 3)$, it may correspond to the dibaryon d^* proposed in the Los Alamos potential model[23], the QDCSM[7, 22, 24, 25] and the Glauber multi-diffraction model[26]. In addition, the presently proposed dibaryon states with $(T, S) = (1, 2), (2, 1)$ may correspond to the narrow dibaryons proposed (with mass 2122 MeV, 2150 MeV, 1956 ± 6 MeV, respectively) in the recent pp scattering experiments[27, 28]. However the experimental data need to be re-analyzed more carefully since similar experiment accomplished most recently[29] does not provide any data to support the result in the other mass region in Ref.[27].

4.2 States with strangeness -5 and -6

It has been known that, when multi-quark system has a large strangeness, the S-wave contribution is dominant. From Table 3, we find that $(s, T, S) = (-5, \frac{1}{2}, 1), (-5, \frac{1}{2}, 0)$ and $(-6, 0, 0)$ are the three lowest states. From Table 2, one can obtain that the $(-6, 0, 0)$ component corresponds mainly to the state $\Omega\Omega$. The lowest states with strangeness -5 , $(-5, \frac{1}{2}, 0)$, is $\Xi^*\Omega$ or a hidden-color state. Another low-lying state, $(-5, \frac{1}{2}, 1)$, would be $\Xi\Omega$ or the coupling of $\Xi\Omega$ and $\Xi^*\Omega$.

From Table 3, one can also recognize that $[\Omega\Omega]_{(0,0^+)}$ has a dominant orbital symmetry $[42]$. Its hidden-color partner, which has the same quantum number (T, S) but a different orbital symmetry [6], might have such a high energy that it cannot be stable. However, it can contribute to the mass of $[\Omega\Omega]_{(0,0^+)}$ in experiment, if its mass is not very large. $[\Xi^*\Omega]_{(1/2,0)}$ also has a low-lying hidden-color partner and the result is the same as $\Omega\Omega$.

After the possibility of the $s = -6$ dibaryon was proposed in SU(3) chiral soli-

ton model[8], more sophisticated calculations in the SU(3) chiral quark model[9] and QDCSM[30] indicate that the $[\Omega\Omega]_{(0,0^+)}$ dibaryon may have binding energy $E_b = 45 \sim 115$ MeV. Recently, the color-singlet $\Xi^*\Omega$ ($S = 0, 3$), $\Xi\Omega$ and their coupling $\Xi^*\Omega$ - $\Xi\Omega$ ($S = 1, 2$) have also been studied in the chiral quark model[13]. It was found that, when $S = 0$, $\Xi^*\Omega$ may be a dibaryon with binding energy $E_b = 80.0 \sim 92.4$ MeV. When $S = 1$, $\Xi\Omega$ may also be a dibaryon with binding energy $E_b = 26.2 \sim 32.9$ MeV. However, up to now, there is still no evidence for the dibaryons with $S = 2$ or 3 to exist[13]. It indicates that $[\Omega\Omega]_{(0,0)}$ and $[\Xi^*\Omega]_{(1/2,0)}$ are deeply bound dibaryon with narrow widths, whereas $[\Xi\Omega]_{(1/2,1)}$ and $[\Xi\Omega$ - $\Xi^*\Omega]_{(1/2,1)}$ are weakly bound only if the chiral field can provide an attraction among the baryons. The present INS analysis result is consistent with these numerical results very well.

It is worth to mention that some of these low-lying states may be hidden-color states. Since the states have large strangeness, it is hard to produce them in proton-proton collisions. However, strangeness production can be enhanced in heavy ion collisions[31], especially at RHIC energies. The dibaryon $[\Omega\Omega]_{(0,0^+)}$ has been suggested as one of the possible signals of quark-gluon plasma(QGP) due to the large gluon density and low energy threshold for $s\bar{s}$ formation[32, 33, 34]. The dibaryons $[\Omega\Omega]_{(0,0^+)}$ and $[\Xi^*\Omega]_{(1/2,0^+)}$ may then be observed in this kind of experiments after careful discussion[9, 30].

4.3 States with strangeness -4

Table 3 indicates that if $s = -4$, the states with $(T, S) = (0, 1)$, $(1, 0)$, $(1, 1)$ and $(1, 2)$ are the four low-lying states. Considering the spin-dependent interaction again, we expect the $(1, 0)$ state to be a stable one. According to Table 2, it is probably the $\Xi\Xi$ or $\Xi^*\Xi^*$ state. Unlike the strangeless state $T(J^\pi) = 1(0^+)$, $\Xi\Xi$ also associates with orbital symmetries $\{5\ 1\}$ and $\{3\ 3\}$ in P-wave resonance. This indicates that $\Xi\Xi$'s energy will not be small enough. The recent SU(3) chiral quark model calculation[35] gave the similar result that it may be a weakly bound state whose binding behavior depends on the contribution of the chiral field. According to Table 2, the $(1, 0)$ state may be the $\Sigma^*\Omega$

state, too. However, until now there is no numerical result of this state. We then suggest that relevant calculation and discussion are necessary.

4.4 States with strangeness -1 , -2 and -3

From Table 3 one can easily recognize that almost all the states with $s = -1, -2, -3$ are associated with the orbital symmetries $[6]$, $[4\ 2]$ and $[2\ 2\ 2]$ except for $(s, T, S) = (-2, 0, 3)$. It is then difficult to rank them.

It has been well known that the six-quark system holds the symmetry $S_6 \otimes SU_{CFS}(18)$. According to group theory, we can classify the quantum states basing on the group reduction $S_6 \otimes SU_C(3) \otimes SU_S(2) \otimes SU_T(2) \otimes U_s(1)$, and obtain the quantum numbers of spin, isospin and strangeness. The states determined in this way are always referred to as in the “symmetry” basis. On the other hand, we can classify the states of the six-quark system in pairs of free baryons(e.g. NN , $\Omega\Omega$ and so on) and hidden-color channel states with explicit quantum numbers. These are referred to as in the “physics” basis. The “symmetry” basis can be transformed into the “physics” basis, and such a transformation causes couplings among the states in “symmetry” basis. When $s = 0, -5$ and -6 , the couplings are simple, the states expressed in the “physics” basis present the main properties of those in the “symmetry” basis. Then the energies of the low-lying “physics” states are much different from each other. Nevertheless, when $s = -1, -2$ and -3 , the couplings are so complicated that many low energy states (with nodeless wave-functions) in the “symmetry” basis contribute to one “physics” state. This makes it difficult to separate each “symmetry” state in experiment, since we can only measure the “physics” one. Meanwhile, due to the coupling, not only low-lying states, but also higher energy states will combine together. In this sense, the fact that the H-particle ($s = -2$) predicted more than 20 years ago has not yet been observed in experiments may be attributed to that several “symmetry” states with higher energies combine in the “physics” state and make its structure much more complicated. In fact, several theoretical and experimental results in the same spirit have been proposed in the last few years. For example, it has been found

that when some minor effects are included, the H dibaryon's mass will raise and become above the $\Lambda\Lambda$ threshold[11, 36, 37]. However, right now we can't conclude that there do not exist stable dibaryon when $s = -1, -2$ and -3 until we get accurate quantitative results about the couplings. After all, we should notice that this is an important effect when we discuss the H particle and other dibaryon with a medium strangeness.

5 The low-lying P-wave states

In view of the baryon-baryon collision, not only the bound states but also the low-lying resonances are important. Moreover, although we have found some states with low energies from the above discussion, we do not have knowledge about whether they are lower than the threshold of open channels. Hence, we can not understand whether they are really bound. Considering the resonance, one knows that the main feature is its width. If the energy is higher than the threshold of open channels, the width is too broad. Then the resonance can not be detected, and the existence of such a resonance is meaningless. When the broadness of the width is taken into account, the relative P-wave collision is even more important than the S-wave collision for creating narrow low-lying resonances, since there exists a centrifugal barrier which would help to keep the orbital wave function in the interior region. Therefore, in addition to the $L = 0$ case having been discussed above, we have to study the case of $L = 1$ as follows.

By calculating the determinants of the matrixes of the homogeneous linear equations (as in Eqs.(8) and (9)) the inherently nodeless components of a six-quark system with $L = 1$ and $\pi_{dib} = -$ can be identified. We obtain then the accessible orbital symmetries as listed in Eq.(11). Accordingly, the favorable components with $L^\pi = 1^-$ and fulfilling all the Eqs.(1)~(4), (8) and (9) are the three having symmetries

$$[f]_O \otimes [f]_C \otimes [f]_{FS} \in \{[5\ 1] \otimes [2\ 2\ 2] \otimes [4\ 2], [3\ 3] \otimes [2\ 2\ 2] \otimes [6], [3\ 3] \otimes [2\ 2\ 2] \otimes [4\ 2]\} .(12a)$$

If we go beyond the constraint in Eq. (4), we have the other possible building blocks of

the P-wave resonance

$$\begin{aligned}
[f]_O \otimes [f]_C \otimes [f]_{FS} \in \{ & [4\ 1\ 1] \otimes [2\ 2\ 2] \otimes [4\ 2], [3\ 2\ 1] \otimes [2\ 2\ 2] \otimes [5\ 1], \\
& [3\ 2\ 1] \otimes [2\ 2\ 2] \otimes [4\ 2], [2\ 2\ 1\ 1] \otimes [2\ 2\ 2] \otimes [4\ 2] \}. \quad (12b)
\end{aligned}$$

This indicates that there may also exist some non-two-baryon states, namely the hidden-color channel states.

Since $L = 1$ states may always have energies larger than $L = 0$ states, we can take the configuration (strangeness, isospin, spin) = (s, T, S) as the possible candidates of P-wave dibaryon only if it accesses to the P-wave component but not to the S-wave one. Looking over Table 4 and Table 3 together, one can recognize that the configurations $(s, T, S) = (-6, 0, 1)$, $(-4, 0, 0)$, $(-2, 0, 3)$, $(0, 0, 0)$, $(0, 0, 2)$, $(0, 2, 0)$, $(0, 1, 3)$, $(0, 3, 1)$ and $(0, 3, 3)$ might be the low energy $L = 1$ states. Taking the Pauli principle into account, we find that the states with the configuration $(s, T, S) = (-4, 0, 0)$, $(0, 0, 0)$, $(0, 0, 2)$, $(0, 2, 0)$, $(0, 1, 3)$, $(0, 3, 1)$ and $(0, 3, 3)$ can decay into two baryons easily. One can thus obtain that there are only two lowest P-wave states: $(T, S) = (0, 1)$ with $s = -6$ and $(T, S) = (0, 3)$ with $s = -2$. Considering the characteristic of the spin-orbital interaction among quarks (see for example Ref.[38]), one can identify that, when the S and L are fixed, the state with higher J may have lower energy. The possible J^π of the above two states may then be 2^- , 4^- , respectively. From Table 2, one can infer that they are the $(\Omega\Omega)_{(0,2^-)}$, $(\Sigma^*\Sigma^*)_{(0,4^-)}$ states and the hidden color channel states with the same quantum numbers.

Even though the configuration $(s, T, S) = (0, 0, 1)$ is accessible to the S-wave component (with multiplicity 5) and its multiplicity to access the P-wave is only 1, it is still worth being discussed, since bag-string model and chiral quark model calculations[4, 5, 39] and some experiments[40] show that there may exist dibaryon state with exotic quantum numbers $L = 1$, $T(J^\pi) = 0(0^-)$ (denoted as d'). Since d' does not obey the Pauli principle, it is a hidden-color channel state and does not simply decay into two baryons. In the present INS analysis, among the seven P-wave $[f]_O \otimes [f]_{FS}$ configurations, only $[3\ 2\ 1] \otimes [5\ 1]$ is the nodeless component accessible to the $(s, T, S) = (0, 0, 1)$ state. The

d' may then not have a low energy due to the emergence of INS. Once d' has low energy, it must hold a dominant component with orbital symmetry $[f]_O = [3\ 2\ 1]$. However, this orbital symmetry has not yet been discussed in the chiral quark model[39]. Moreover, the QDCSM calculation indicates that the dibaryon d' may involve more complicated structure[41]. Then, more careful investigations may be interesting to check the existence of d' further.

Since spin-dependent quark-quark interactions can lower the energy of the excited s^4p^2 state and raise the energy of the s^6 state[39], the dibaryon states d^* (with $T(J^\pi) = 0(3^+)$)[7, 22, 23, 24, 25, 26] and d' are considered to have energies lower than S-wave $(T, S) = (1, 0)$ state. In view of that all the $s = 0$ states are very near the $\pi\pi$ threshold, one could easily reach a conclusion that, except for the deuteron, all of the S-wave dibaryons with $s = 0$ have energies higher than d' . However, the inelastic scattering experiments $pp \Rightarrow p\pi^+X$ [27], $pp \Rightarrow X\gamma\gamma$ [28] and quasielastic-charge-exchange experiment $p\alpha \Rightarrow nppd$, $pppn$ [42] give very slight evidence for narrow dibaryon d' , and the quantum numbers $(T, J^\pi) = (0, 0^-)$ for d' should be carefully reexamined[27]. Furthermore, the most recent $pp \Rightarrow pp\pi^+\pi^-$ measurements[29] indicates that the so called dibaryon d' may not exist at all. The result of very small accessibility obtained in the present analysis may provide a reason to understand such a contradiction. In contrast, the large accessibility of the $(T, S) = (0, 3)$ state discussed in the last section provides a clue that the d^* dibaryon may be observed in experiment.

Referring the states with large accessibility as the states favorable to binding, we obtain finally the candidates of low-lying dibaryons from the above discussion. The results are listed in Table 5.

6 Summary and Remarks

We have studied a kind exotic QCD state, namely the dibaryon states, in this paper. Taking the dibaryons as six-quark clusters with u , d and s quarks, we have discussed the symmetries of the states. After investigating the inherent nodal surface of the system

based on symmetry analysis, we obtain the quantum numbers of the low-lying S-wave and P-wave states. Meanwhile the hidden-color channel states are discussed. It shows that although several states with strangeness $s = 0$ may have low energy, there is probably no stable S-wave dibaryon except deuteron. If the strangeness is large, however, there may exist stable dibaryon states. $[\Omega\Omega]_{(0,0+)}$, $[\Xi^*\Omega]_{(1/2,0+)}$, $[\Xi^*\Omega]_{(1/2,1+)}$ and $[\Xi\Omega]_{(1/2,1+)}$ are proposed to be the candidates of stable dibaryons. $[\Xi\Omega-\Xi^*\Omega]_{(1/2,1+)}$ and $[\Xi\Xi]_{(1,0+)}$ are low-lying states, too. However, they may be not stable enough. We also find that two important P-wave resonances $(s, T, S) = (-6, 0, 1)$, $(-2, 0, 3)$ may be stable and have low energy. Nevertheless, the d' with $(s, T, S) = (0, 0, 1)$ is not a favorite candidate of dibaryon in the present analysis. It is evident that these results agree very well with those obtained in various numerical calculations and experimental observations. In the case that $s = -1$, -2 and -3 , it is difficult to determine the low-lying states since many such kind states are associated with each other. This kind mixing may be the reason for that the H-particle has not yet been observed in experiment convincingly.

Combining our present analysis and the previous numerical calculations, we conclude that the S-wave dibaryon states $[\Omega\Omega]_{(0,0)}$ and $[\Xi^*\Omega]_{(1/2,0)}$ may be observed in the RHIC experiments since they are the stable low-lying states. Meanwhile, the P-wave states $[\Omega\Omega]_{(0,2-)}$ and $[\Sigma^*\Sigma^*]_{(0,4-)}$ may also be observed as the dibaryon candidates. Since all of them may contain hidden-color channel state couplings, we propose that observing the states with hidden-color channels may be an appropriate branch to explore dibaryon states. In addition, the dibaryon d^* may also be observed in experiment.

Finally, it is remarkable that the presently proposed INS analysis approach is just a mathematical realization of the intrinsic property of the underlying physics. No dynamics is included at all. The results obtained are then model independent. However, it can give only qualitative predictions. To obtain concrete knowledge about dibaryon states, for instance their binding energies, decay widths, one should implement dynamical calculations definitely. Therefore, combining the dynamical calculation and INS analysis together is much more efficient in exploring dibaryons and other multi-quark cluster states.

This work is supported by the National Science Foundation of China with Grant Nos. 10075002, 10135030, 19875001, 90103028. One of the authors (YXL) thanks also the support by the Major State Key Basis Research Programme under Contract No. G2000077400 and the Foundation for University Key Teacher by the Ministry of Education, China.

References

- [1] A. Chodos, R. L. Jaffe, K. Jonson, C. B. Thorn, and V. F. Weisskopf, Phys. Rev. **D 9**, 3471 (1974).
- [2] H. Kanada *et.al.* Nucl. Phys. **A 444**, (1985) 209
- [3] R. L. Jaffe, Phys. Rev. Lett. **38**, 195 (1977).
- [4] P. J. Mulders, A. T. Aerts, and J. J. de Swarts, Phys. Rev. **D 21**, 2653 (1980).
- [5] L. A. Kondratyuk, B. B. Martemyanov, and M. G. Schepkin, Sov. J. Nucl. Phys. **45**, 776 (1987).
- [6] T. Goldman, K. Maltman, G. J. Stephenson, Fr., K. E. Schmidt, and F. Wang, Phys. Rev. Lett. **59**, 627 (1987).
- [7] F. Wang, J. L. Ping, G. H. Wu, L. J. Teng, and T. Goldman, Phys. Rev. **C 51**, 3411 (1995).
- [8] V. B. Kopeliovich, B. Schwesinger, and B. E. Stern, Phys. Lett. **B 242**, 145 (1990);
V. B. Kopeliovich, Nucl. Phys. **A 639**, 75 (1998).
- [9] Z. Y. Zhang, Y. W. Yu, C. R. Ching, T. H. Ho, and Z. D. Lu, Phys. Rev. **C 61**, 065204 (2000).
- [10] N. Kodama, M. Oka, and T. Hatsuda, Nucl. Phys. **A 580**, (1994) 445.
- [11] J. W. Negele, A. Pochinsky, B. Scarlet, Nucl. Phys. **B (Proc. Supl.) 73**, (1999) 255.
- [12] M. Harvey, Nucl. Phys. **A 352**, 301 (1981).
- [13] Q. B. Li, P. N. Shen, Phys. Rev. **C 62**, 028202 (2000).
- [14] R. W. Stotzer, *et al.*, Phys. Rev. Lett. **78**, 3646 (1997).
- [15] Y. Suzuki, Nucl. Phys. **A 444**, 637 (1985).

- [16] C. G. Bao, *Few-Body Syst.* **13**, 41 (1992); *Phys. Rev. A* **47**, 1752 (1993); *Phys. Rev. A* **50**, 2182 (1994); *Chin. Phys. Lett.* **14**, 20 (1997); *Phys. Rev. Lett.* **79**, 3475 (1997); *Phys. Lett. A* **250**, 123 (1999).
- [17] C. G. Bao, *Nucl. Phys. A* **637**, 520 (1998).
- [18] C. G. Bao, Y. X. Liu, *Phys. Rev. Lett.* **82**, 61 (1999).
- [19] J. Q. Chen, *Group Representation Theory for Physicists* (World Scirntific, Singapore, 1989)
- [20] D. R. Tilley, C. M. Cheves, J. L. Godwin, G. M. Hale, H. M. Hofmann, J. H. Kelley, C. G. Sheu, and H. R. Weller, *Nucl. Phys. A* **708**, 3 (2002).
- [21] F. Wang, G. H. Wu, L. J. Teng, and T. Goldman, *Phys. Rev. Lett.* **69**, 2901 (1992).
- [22] J. L. Ping, F. Wang, T. Goldman, *Nucl. Phys. A* **657**, 95 (1999).
- [23] T. Goldman, K. Maltman, G. J. Stephenson, Fr., K. E. Schmidt, and F. Wang, *Phys. Rev. C* **39**, 1889 (1989).
- [24] J. L. Ping, F. Wang, T. Goldman, *Nucl. Phys. A* **688**, 871 (2001).
- [25] J. L. Ping, H. R. Pang, F. Wang, T. Goldman, *Phys. Rev. C* **65**, 044003 (2002).
- [26] C. W. Wong, *Phys. Rev. C* **57**, 1962 (1998).
- [27] B. Tatischeff, *et. al.*, *Phys. Rev. C* **59**, 1878 (1999).
- [28] A. S. Khrykin, *et.al.*, *Phys. Rev. C* **64**, 034002 (2001); A. S. Khrykin, *nucl-ex/0211034v3*.
- [29] W. Brodowski, *et al.*, *Phys. Lett. B* **550**, 147 (2002).
- [30] H. R. Pang, J. L. Ping, F. Wang, and T. Goldman, *Phys. Rev. C* **66**, 025201 (2002).
- [31] T. A. Armstrong, *et. al.*, *Phys. Rev. C* **63**, 054903 (2001).

- [32] J. Rafelski, B. Müller, Phys. Lett. **B 101**, 111 (1982).
- [33] P. Koch, B. Müller, J. Rafelski, Phys. Rep. **142**, 67 (1986).
- [34] S. Pal, C. M. Ko, Z. Y. Zhang, nucl-th/0107070
- [35] P. N. Shen, Q. B. Li, Z. Y. Zhang, and Y. W. Yu, Nucl. Phys. **A 675**, 234 (2000).
- [36] P. N. Shen, Z. Y. Zhang, Y. W. Yu, X. Q. Yuan, and S. Yang, J. Phys. **G 25**, 1807 (1999).
- [37] M. Oka, Hyperfine Interaction **103**, 275 (1996).
- [38] Y. W. Yu, Z. Y. Zhang, P. N. Shen, and L. R. Dai, Phys. Rev. **C 52**, 3393 (1995).
- [39] A. J. Buchmann, G. Wagner, A. Faessler, Phys. Rev. **C 57**, 3340 (1998).
- [40] R. Bilger, H. A. Clement, and M. G. Scgepkin, Phys. Rev. Lett. **71**, 42 (1993); R. Bilger, Nucl. Phys. **A 629**, 141 (1998).
- [41] J. L. Ping, F. Wang, T. Goldman, Phys. Rev. **C 62**, 054007 (2000).
- [42] A. V. Blinov, M. V. Chadeyeva, V. F. Turov, Phys. Atom. Nucl. **64**, 907 (2001)

Table 1: The flavor-spin symmetries corresponding to each possible orbital symmetry with color singlet restriction.

Orbital (S_6)	$SU(6)_{FS}$
[6]	[3 3]*
[5 1]	[4 2]*, [3 2 1]
[4 2]	[5 1]*, [4 1 1], [3 3]*, [3 2 1], [2 2 1 1]
[4 1 1]	[4 2]*, [4 1 1], [3 2 1], [2 2 1 1]
[3 3]	[6]*, [4 2]*, [3 1 ³], [2 2 2]
[3 2 1]	[5 1]*, [4 2]*, [4 1 1], [3 1 ³], [3 2 1] ² , [2 2 1 1], [2 1 ⁴]
[3 1 ³]	[4 1 1], [3 3]*, [3 2 1], [3 1 ³], [2 2 1 1]
[2 2 2]	[4 1 1], [3 3]*, [3 1 ³], [2 2 1 1], [1 ⁶]
[2 2 1 1]	[4 2]*, [3 1 ³], [2 2 2]
[2 1 ⁴]	[3 2 1], [2 2 1 1]
[1 ⁶]	[2 2 2]

Table 2: Classification of the states with asterisks in table 1

strange	states	(isospin, spin)
0	N^2	(0, 0), (0, 1), (1, 0), (1, 1)
	Δ^2	(0, 0), (0, 1), (0, 2), (0, 3), (1, 0), (1, 1), (1, 2), (1, 3), (2, 0), (2, 1), (2, 2), (2, 3), (3, 0), (3, 1), (3, 2), (3, 3),
	$N\Delta$	$(1, 1)^2, (1, 2)^2, (2, 1)^2, (2, 2)^2$
	CC	(0, 0), (0, 1), (0, 2), (0, 3), (1, 0), (1, 1) ² , (1, 2) ² , (1, 3), (2, 0), (2, 1) ² , (2, 2), (3, 0), (3, 1),
-1	$N\Lambda$	$(1/2, 0)^2, (1/2, 1)^2$
	$N\Sigma$	$(3/2, 0)^2, (3/2, 1)^2, (1/2, 0)^2, (1/2, 1)^2$
	$N\Sigma^*$	$(3/2, 1)^2, (3/2, 2)^2, (1/2, 1)^2, (1/2, 2)^2$
	$\Delta\Lambda$	$(3/2, 1)^2, (3/2, 2)^2$
	$\Delta\Sigma$	$(5/2, 1)^2, (5/2, 2)^2, (3/2, 1)^2, (3/2, 2)^2, (1/2, 1)^2, (1/2, 2)^2$
	$\Delta\Sigma^*$	$(5/2, 0)^2, (5/2, 1)^2, (5/2, 2)^2, (5/2, 3)^2, (3/2, 0)^2, (3/2, 1)^2,$ $(3/2, 2)^2, (3/2, 3)^2, (1/2, 0)^2, (1/2, 1)^2, (1/2, 2)^2, (1/2, 3)^2$
	CC	$(1/2, 0)^3, (1/2, 1)^6, (1/2, 2)^5, (1/2, 3)^2, (3/2, 0)^3, (3/2, 1)^6,$ $(3/2, 2)^4, (3/2, 3), (5/2, 0)^2, (5/2, 1)^3, (5/2, 2), (5/2, 3)$
-2	Λ^2	(0, 0), (0, 1)
	Σ^2	(0, 0), (0, 1), (1, 0), (1, 1)
	Σ^{*2}	(0, 0), (0, 1), (0, 2), (0, 3), (1, 0), (1, 1), (1, 2), (1, 3)
	$\Sigma^*\Sigma$	$(0, 1)^2, (0, 2)^2, (1, 1)^2, (1, 2)^2$
	$N\Xi$	$(0, 0)^2, (0, 1)^2, (1, 0)^2, (1, 1)^2$
	$N\Xi^*$	$(0, 1)^2, (0, 2)^2, (1, 1)^2, (1, 2)^2$
	$\Delta\Xi$	$(1, 1)^2, (1, 2)^2, (2, 1)^2, (2, 2)^2$
	$\Delta\Xi^*$	$(1, 0)^2, (1, 1)^2, (1, 2)^2, (1, 3)^2, (2, 0)^2, (2, 1)^2, (2, 2)^2, (2, 3)^2$
	CC	(0, 0), (0, 1) ⁴ , (0, 2) ⁴ , (0, 3), (1, 0) ⁷ , (1, 1) ⁴ , (1, 2) ⁹ , (1, 3) ² , (2, 0) ⁵ , (2, 1) ⁹ , (2, 2) ⁵ , (2, 3) ²

(Table 2 continued)

strange	states	(isospin, spin)
-3	$N\Omega$	$(1/2, 1)^2, (1/2, 2)^2$
	$\Delta\Omega$	$(3/2, 0)^2, (3/2, 1)^2, (3/2, 2)^2, (3/2, 3)^2$
	$\Lambda\Xi$	$(1/2, 0)^2, (1/2, 1)^2$
	$\Lambda\Xi^*$	$(1/2, 1)^2, (1/2, 2)^2$
	$\Sigma\Xi$	$(1/2, 0)^2, (1/2, 1)^2, (3/2, 0)^2, (3/2, 1)^2$
	$\Sigma^*\Xi$	$(1/2, 1)^2, (1/2, 2)^2, (3/2, 1)^2, (3/2, 2)^2$
	$\Sigma\Xi^*$	$(1/2, 1)^2, (1/2, 2)^2, (3/2, 1)^2, (3/2, 2)^2$
	$\Sigma^*\Xi^*$	$(1/2, 0)^2, (1/2, 1)^2, (1/2, 2)^2, (1/2, 3)^2,$ $(3/2, 0)^2, (3/2, 1)^2, (3/2, 2)^2, (3/2, 3)^2$
CC	$(1/2, 0)^6, (1/2, 1)^9, (1/2, 2)^5, (1/2, 3),$ $(3/2, 0)^5, (3/2, 1)^6, (3/2, 2)^3, (3/2, 3)^2$	
-4	$\Lambda\Omega$	$(0, 1)^2, (0, 2)^2$
	$\Sigma\Omega$	$(1, 1)^2, (1, 2)^2$
	$\Sigma^*\Omega$	$(1, 0)^2, (1, 1)^2, (1, 2)^2, (1, 3)^2$
	Ξ^2	$(0, 0), (0, 1), (1, 0), (1, 1)$
	$\Xi^*\Xi$	$(0, 1)^2, (0, 2)^2, (1, 1)^2, (1, 2)^2$
	Ξ^{*2}	$(0, 0), (0, 1), (0, 2), (0, 3), (1, 0), (1, 1), (1, 2), (1, 3)$
CC	$(0, 0)^2, (0, 1)^4, (0, 2)^4, (1, 0)^3, (1, 1)^6, (1, 2)^3, (1, 3)$	
-5	$\Omega\Xi$	$(1/2, 1)^2, (1/2, 2)^2$
	$\Omega\Xi^*$	$(1/2, 0)^2, (1/2, 1)^2, (1/2, 2)^2, (1/2, 3)^3$
	CC	$(1/2, 0)^2, (1/2, 1)^3, (1/2, 2)$
-6	Ω^2	$(0, 0), (0, 1), (0, 2), (0, 3)$
	CC	$(0, 0), (0, 1)$

Table 3: Multiplicity of the accessibility of the S-wave nodeless components $[f]_O \otimes [f]_{FS}$

s	S	T	$[6] \otimes [33]$	$[42] \otimes [51]$	$[42] \otimes [33]$	$[222] \otimes [33]$
0	0	0	0	0	0	0
	0	1	1	1	1	1
	0	2	0	0	0	0
	0	3	1	0	1	1
	1	0	1	1	1	1
	1	1	0	1	0	0
	1	2	1	1	1	1
	1	3	0	0	0	0
	2	0	0	0	0	0
	2	1	1	1	1	1
	2	2	0	1	0	0
	2	3	0	1	0	0
	3	0	1	0	1	1
	3	1	0	0	0	0
	3	2	0	1	0	0
	3	3	0	0	0	0
-1	0	1/2	1	2	1	1
	0	3/2	1	1	1	1
	0	5/2	1	0	1	1
	1	1/2	2	3	2	2
	1	3/2	2	3	2	2
	1	5/2	1	1	1	1
	2	1/2	2	1	2	2
	2	3/2	1	3	1	1
	2	5/2	0	2	0	0
	3	1/2	1	0	1	1
	3	3/2	0	1	0	0
	3	5/2	0	1	0	0

(Table 3 continued)

s	S	T	$[6] \otimes [33]$	$[42] \otimes [51]$	$[42] \otimes [33]$	$[222] \otimes [33]$
-2	0	0	2	2	2	2
	0	1	1	2	1	1
	0	2	2	1	2	2
	1	0	1	2	1	1
	1	1	4	5	4	4
	1	2	1	2	1	1
	2	0	2	1	2	2
	2	1	2	3	2	2
	2	2	1	2	1	1
	3	0	0	0	0	0
	3	1	1	1	1	1
	3	2	0	1	0	0
-3	0	1/2	1	2	1	1
	0	3/2	2	1	2	2
	1	1/2	3	4	3	3
	1	3/2	2	3	2	2
	2	1/2	2	3	2	2
	2	3/2	1	3	1	1
	3	1/2	0	1	0	0
	3	3/2	1	1	1	1
-4	0	0	0	0	0	0
	0	1	2	1	2	2
	1	0	2	2	2	2
	1	1	1	2	1	1
	2	0	0	2	0	0
	2	1	1	3	1	1
	3	0	0	1	0	0
	3	1	0	1	0	0

(Table 3 continued)

s	S	T	$[6] \otimes [33]$	$[42] \otimes [51]$	$[42] \otimes [33]$	$[222] \otimes [33]$
-5	0	1/2	1	0	1	1
	1	1/2	1	1	1	1
	2	1/2	0	2	0	0
	3	1/2	0	1	0	0
-6	0	0	1	0	1	1
	1	0	0	0	0	0
	2	0	0	1	0	0
	3	0	0	0	0	0

Table 4: Multiplicity of the accessibility of the P-wave nodeless components $[f]_O \otimes [f]_{FS}$

s	S	T	$[5\ 1] \otimes [4\ 2]$	$[4\ 1\ 1] \otimes [4\ 2]$	$[3\ 3] \otimes [6]$	$[3\ 3] \otimes [4\ 2]$	$[3\ 2\ 1] \otimes [5\ 1]$	$[3\ 2\ 1] \otimes [4\ 2]$	$[2\ 2\ 1\ 1] \otimes [4\ 2]$
0	0	0	1	1	1	1	0	1	1
	0	1	0	0	0	0	1	0	0
	0	2	1	1	0	1	0	1	1
	0	3	0	0	0	0	0	0	0
	1	0	0	0	0	0	1	0	0
	1	1	2	2	1	2	1	2	2
	1	2	1	1	0	1	1	1	1
	1	3	1	1	0	1	0	1	1
	2	0	1	1	0	1	0	1	1
	2	1	1	1	0	1	1	1	1
	2	2	1	1	1	1	1	1	1
	2	3	0	0	0	0	1	0	0
	3	0	0	0	0	0	0	0	0
	3	1	1	1	0	1	0	1	1
	3	2	0	0	0	0	1	0	0
3	3	0	0	1	0	0	0	0	
-1	0	1/2	2	2	1	2	2	2	2
	0	3/2	2	2	0	2	1	2	2
	0	5/2	1	1	0	1	0	1	1
	1	1/2	4	4	1	4	3	4	4
	1	3/2	4	4	1	4	3	4	4
	1	5/2	2	2	0	2	1	2	2
	2	1/2	3	3	0	3	1	3	3
	2	3/2	3	3	1	3	3	3	3
	2	5/2	1	1	1	1	2	1	1
	3	1/2	1	1	0	1	0	1	1
	3	3/2	1	1	0	1	1	1	1
3	5/2	0	0	1	0	1	0	0	

(Table 4 continued)

s	S	T	$[5\ 1] \otimes [4\ 2]$	$[4\ 1\ 1] \otimes [4\ 2]$	$[3\ 3] \otimes [6]$	$[3\ 3] \otimes [4\ 2]$	$[3\ 2\ 1] \otimes [5\ 1]$	$[3\ 2\ 1] \otimes [4\ 2]$	$[2\ 2\ 1\ 1] \otimes [4\ 2]$
-2	0	0	1	1	0	1	2	1	1
	0	1	4	4	1	4	2	4	4
	0	2	1	1	0	1	1	1	1
	1	0	4	4	1	4	2	4	4
	1	1	6	6	1	6	5	6	6
	1	2	4	4	1	4	2	4	4
	2	0	2	2	0	2	1	2	2
	2	1	5	5	1	5	3	5	5
	2	2	2	2	1	2	2	2	2
	3	0	1	1	0	1	0	1	1
	3	1	1	1	0	1	1	1	1
-3	0	1/2	3	3	0	3	2	3	3
	0	3/2	2	2	1	2	1	2	2
	1	1/2	6	6	1	6	4	6	6
	1	3/2	4	4	1	4	3	4	4
	2	1/2	4	4	1	4	3	4	4
	2	3/2	3	3	1	3	3	3	3
	3	1/2	1	1	0	1	1	1	1
	3	3/2	1	1	1	1	1	1	1
-4	0	0	2	2	0	2	0	2	2
	0	1	1	1	0	1	1	1	1
	1	0	2	2	0	2	2	2	2
	1	1	4	4	1	4	2	4	4
	2	0	2	2	1	2	2	2	2
	2	1	2	2	1	2	3	2	2
	3	0	0	0	0	0	1	0	0
	3	1	1	1	1	1	1	1	1

(Table 4 continued)

s	S	T	$[51] \otimes [42]$	$[411] \otimes [42]$	$[33] \otimes [6]$	$[33] \otimes [42]$	$[321] \otimes [51]$	$[321] \otimes [42]$	$[2211] \otimes [42]$
-5	0	1/2	1	1	0	1	0	1	1
	1	1/2	1	1	0	2	1	2	2
	2	1/2	2	1	1	1	2	1	1
	3	1/2	0	0	1	0	1	0	0
-6	0	0	0	0	0	0	0	0	0
	1	0	1	1	0	1	0	1	1
	2	0	0	0	0	0	1	0	0
	3	0	0	0	1	0	0	0	0

Table 5: Quantum numbers of the candidates of low-lying dibaryons with $L = 0$ and $L = 1$

s	S	T	L	π	J	$[f]_O \otimes [f]_{FS}$
0	1	0	0	+	1	$[6] \otimes [33], [42] \otimes [51], [42] \otimes [33], [222] \otimes [33]$
0	3	0	0	+	3	$[6] \otimes [33], [42] \otimes [33], [222] \otimes [33]$
0	0	1	0	+	0	$[6] \otimes [33], [42] \otimes [51], [42] \otimes [33], [222] \otimes [33]$
-5	0	$\frac{1}{2}$	0	+	0	$[6] \otimes [33], [42] \otimes [33], [222] \otimes [33]$
-5	1	$\frac{1}{2}$	0	+	1	$[6] \otimes [33], [42] \otimes [51], [42] \otimes [33], [222] \otimes [33]$
-6	0	0	0	+	0	$[6] \otimes [33], [42] \otimes [33], [222] \otimes [33]$
-2	3	0	1	-	2, 3, 4	$[51] \otimes [42], [411] \otimes [42], [33] \otimes [42], [321] \otimes [42], [2211] \otimes [42]$
-6	1	0	1	-	0, 1, 2	$[51] \otimes [42], [411] \otimes [42], [33] \otimes [42], [321] \otimes [42], [2211] \otimes [42]$